

Dynamic modelling of the secondary drying stage of freeze-drying reveals distinct desorption kinetics for bound water

Ioan Cristian Trelea¹, Fernanda Fonseca², Stéphanie Passot¹

¹AgroParisTech, UMR782 Génie et Microbiologie des Procédés Alimentaires

1 av. Lucien Brétignières, F-78850 Thiverval-Grignon, France

²INRA, UMR782 Génie et Microbiologie des Procédés Alimentaires

1 av. Lucien Brétignières, F-78850 Thiverval-Grignon, France

Correspondence to be send to : cristian.trelea@agroparistech.fr, +33(0)130815490 (I.C. Trelea)

Abstract

In freeze-drying, the desorption step for reaching a low target moisture content may take a significant fraction of the total process duration. Since the long term stability of freeze-dried biological products strongly depends on the current moisture content, modelling the desorption process may help safely optimise the secondary drying step. Most published models assume a first-order desorption kinetic, but experimental evidence shows that strongly bound water in the monolayer takes a much longer time to be desorbed than less bound water in multilayer. The proposed model for desorption of freeze-dried lactic acid bacteria preparation accounts for monolayer and multilayer water state in the solid matrix, with very different desorption kinetics. Results showed that the ratio of characteristic desorption times (monolayer/multilayer) was almost 30. Temperature dependence was adequately described by an Arrhenius law in the range of 15 to 40°C. Model parameter identification used simultaneously gravimetric measurements with high time resolution and direct Karl-Fisher titration, from several experiments at different, time-varying temperatures.

Keywords: lyophilisation, desorption kinetic, lactic acid bacteria

Running title: Dynamic model with distinct desorption kinetics

Introduction

Freeze-drying (lyophilisation) is widely used for stabilisation of biological material and pharmaceuticals, such as proteins, vaccines, bacteria, mammal cells and high quality food.[1, 2] It is known to preserve the quality of the dried product (biological, nutritional, organoleptic properties) by freezing the material and promoting the transition of the solvent, usually water, from solid to the

gas phase by sublimation. An interconnected porous structure is created which can be easily rehydrated. Freeze-drying is a time and energy consuming process, currently limited to high added-value products. A lot of research was devoted to its optimisation, often based on mathematical modelling.[3, 4, 5, 6, 7, 8]

Freeze-drying process consists of three main steps: freezing, ice removal by sublimation (primary drying) and unfrozen water removal by desorption from the solid matrix (secondary drying). While most attention was devoted to the optimisation of the first two steps,[7, 9, 10, 11, 12, 13] secondary drying may occupy a significant fraction of the process duration, especially if low moisture content is desired for the final product. The moisture content achieved at the end of the secondary drying is a critical parameter because it governs the long term stability of the product and its shelf life. For pharmaceutical products, target moisture contents as low as 0.01 or 0.02 kg water/kg solids or lower are common,[1] even if it has been shown that over-drying may be detrimental to product quality in some cases.[14, 15, 16, 17, 18] These values may be lower than the monolayer moisture content, requiring the desorption of highly bound water molecules, which is potentially slow.[19]

It is usually considered that water is present in solid matrices in three different forms, corresponding to three more or less arbitrarily defined regions of the sorption isotherm.[20] In the first region, roughly corresponding to water activity values less than 0.2, water molecules form a monolayer, are tightly bound to the solid matrix through hydrogen bonding and are unavailable for reaction. In the second region, for water activities between 0.2 and 0.5, water is loosely bound forming a multilayer. In this case, water molecules can no longer form hydrogen bonds with the glassy solid and water-water interactions become predominant, thereby favouring the formation of microscopic regions of condensed water, such that chemical species can dissolve, diffuse and react. The third region corresponds to water activities higher than 0.5 or 0.6; water is relatively free, exists in capillaries and obeys Raoult's law. In the secondary drying step of the freeze-drying process, residual water mainly corresponds to the first two regions of the sorption isotherm since free water crystallized out in the freezing step and was already eliminated in the primary drying step by sublimation.

Another important parameter governing long term stability of biological products is the maintenance of the solid glassy state. The physicochemical properties of the glassy state (i.e., molecular mobility, stickiness, viscosity changes, structural collapse, crystallization, etc.) are functions of hydration. For a glassy formulation stored below its T_g , reaction rate is lower at low water contents, because the diffusion and mobility of reactants are limited. As water content increases, to a level sufficient to depress the formulation's T_g to a temperature below the storage temperature (i.e. the system becomes rubbery), diffusion limited reactions are accelerated by the increased molecular mobility of reactants and product stability is decreased.

In the context of product stabilisation by freeze-drying, several studies have been devoted to the investigation of rate-limiting mechanisms of water desorption. Pikal *et al.*[21] considered several assumptions concerning the mechanisms of moisture desorption in freeze-drying for both amorphous and crystalline solutions, with different specific solid-gas contact areas. Desorption kinetics determined with a microbalance in various shelf temperature and chamber pressure operating conditions suggested that the rate-limiting step was either evaporation at the solid-gas interface or diffusion in the solid. Liapis and Bruttini[22] also investigated several water removal mechanisms in secondary drying: (1) simultaneous adsorption and desorption at the interface

between the solid (surface of pores) and gas, (2) convective transport in pores, (3) gas diffusion in pores, (4) diffusion of water in the solid particles and (5) diffusion of water on the surface of the solid. They concluded that the first three mechanisms were rate-limiting in the considered amorphous systems. Sadikoglu and Liapis[23] investigated the possibility of desorption model discrimination based on comparison of model predictions with experimental data and highlighted the fact that different rate limiting mechanisms such as solid film mass transfer and surface desorption can lead to equally good agreement with measured residual moisture kinetics.

A pioneering work involving dynamic modelling of the secondary freeze-drying stage for process optimisation is due to Millman *et al.*[24] Their model assumed a one-dimensional top-down movement of the sublimation interface and temperature and moisture distribution in the porous layer. Moisture content profiles in the porous product layer at the end of the primary and secondary drying stages were calculated under various assumptions of heat transfer modes at the top and bottom of the product. Operating condition optimisation (chamber pressure and shelf temperature) were performed based on a target final moisture content of the product and on maximum allowed product temperature constraints. The shortest achievable process time appeared to depend significantly on the selected termination criterion, involving either the average or the maximum moisture content in the dry layer and thus highlighting the need for a comprehensive modelling of the secondary drying. Based on a previously developed model,[23] Sadikoglu *et al.*[3] investigated dynamic optimisation of the freeze-drying process, including the secondary drying stage. They minimised the process duration by allowing time varying shelf temperature and chamber pressure profiles which satisfy maximum allowable product temperature constraints in critical locations and a final product moisture requirement. Results demonstrated significant process duration and final moisture gradient reduction allowed by dynamic optimisation. Liapis and Bruttini[25] extended previous models to freeze-drying in vials by considering a two-dimensional (axial and radial) movement of the sublimation interface and distribution of temperature and moisture in the porous product. Based on this model, Sadikoglu[26] calculated optimal control policies for freeze-drying in vials, with relatively similar conclusions to those derived using the one-dimensional model.[3] Gan *et al.*[27] used a two-dimensional heat and mass transfer model to optimise freeze-drying in vials taking into account the position of the vial on the shelf and the geometric arrangement of the vials. They confirmed that optimal time-varying operating policies that minimise process duration while satisfying product temperature and final moisture constraints also improve intra-vial and inter-vial homogeneity in terms of temperature and residual moisture. This study also provided indications on the number and locations of vials to be monitored in real time to ensure desired product stability and quality.

More recently, Velardi and Barresi[6] addressed the development of simplified dynamic models of the freeze-drying process suitable for on-line monitoring, optimisation and control. In-line control of the process aiming at continuously maintaining the product temperature at its maximum allowable value achieved significant reduction of process time compared to constant operating conditions.[28] Pisano *et al.*[7] compared two control strategies, based on feedback and a simplified dynamic model. They demonstrated the effectiveness of the proposed methods in a wide range of operating conditions, including abrupt changes, and their robustness to possibly incorrect values of model parameters, such as the heat transfer coefficient. Fissore *et al.*[29] focused on the use of a dynamic desorption model as a software sensor to monitor the secondary drying, by coupling the model to a measurement of desorption rate. They were able to estimate in real time the residual amount of

water at the end of the primary drying, the evolution of the product moisture during the secondary drying and the time remaining to reach the target moisture content. Pressure rise, a tool traditionally used in primary drying, was adapted to monitor the desorption process in secondary drying[30] allowing the determination of the residual moisture content of the product and of the desorption kinetic parameter in real time. This study[30] also extended the concepts of quality by design and design space to secondary drying. Accounting for the heterogeneity among the vials in a batch allows the calculation of optimal time evolution of the control variable for the critical (instead of the average) vials and thus improve overall product quality and safety.

In all these investigations the dynamic model of the freeze-drying process, including the desorption model, plays a central role. The results of all model-based off-line and on-line optimisations, monitoring and control procedures, and ultimately the process operation costs and the final product quality, critically depend on the accuracy of the model predictions. The aim of the present study is to develop a dynamic model able to accurately describe the desorption process at very low moisture contents encountered towards the end of the secondary drying. It has been shown for a long time[21] that secondary drying proceeds along at least two different kinetics, associated to different states of water molecules and limiting mass transfer mechanisms. A fast desorption is observed in the first hours and a much slower one when the residual moisture content becomes low. Despite this early observation, most developed mathematical models of the secondary drying stage still assume a single desorption kinetic.[31, 32, 33, 34] Failure to consider the increase in the desorption time when approaching monolayer could lead to the design of over-optimistic secondary drying protocols, especially if automatic model-based optimisation is used. Indeed, underestimating the residual moisture content leads to an overestimation of the critical product temperature, which is usually close to the glass transition temperature of amorphous products, and strongly depends on the current moisture content. Increasing product temperature above this critical value leads to cake shrinkage and collapse, and ultimately to rejection of the batch [35]. As an additional limitation of many of the currently used freeze-drying models, it can be noted that, apart few exceptions,[30] temperature dependence of the desorption kinetics is not taken into account.[5, 6, 23, 26, 31, 36] Temperature was recognised long ago to be a major factor in secondary drying, however,[21] and is common freeze-drying practice to increase temperature to accelerate desorption.

The present study experimentally investigates this temperature dependence and gives a quantitative description. In order to develop a dynamic model useful for process optimisation, the adopted approach was to measure water desorption in secondary drying with adequate experimental tools, allowing sufficient time resolution to put in evidence various drying kinetics. Significantly different desorption kinetics for water molecules with different degrees of association to the solid matrix were accounted for in the model, as well as temperature dependence of the desorption rate.

Materials and methods

Preparation of the freeze-dried bacterial samples

The lactic acid bacteria strain, *Lactobacillus bulgaricus* ssp. *delbrueckii* CFL1, was obtained from the stock culture of the Laboratoire de Génie et Microbiologie des Procédés Alimentaires (INRA, Thiverval-Grignon, France). Concentrated suspensions of lactic acid bacteria were produced by fermentation in controlled conditions of pH (pH = 5.5) and temperature (42°C) as previously

described [18]. After concentration, the bacterial cells were re-suspended in a protective medium, with a weight ratio 1:2 of cells:protective medium. The protective medium was composed of 200 g/L of sucrose and 0.15 M of NaCl. The protected bacterial suspension was aliquoted either into 50 mm diameter stainless steel container (15 mL filled volume) for sorption isotherm and state diagram experiments or into 7 mL glass vials (5 mL filled volume) for the desorption kinetic experiments. The samples were frozen at -80°C in a cold air chamber and then transferred to a pre-cooled shelf at -50°C in a SMH 90 freeze-dryer (Usifroid, Maurepas, France). After a holding step of 1h at -50°C, the chamber pressure was decreased to 20 Pa and the shelf temperature was increased to -20°C at 0.25°C/min to initiate the sublimation phase. After 40h of sublimation, the shelf temperature was increased to 25°C at 0.25°C/min to initiate the desorption phase. After 10h of desorption, the vacuum was broken by injection of air and the samples were packed under vacuum in aluminium bags and stored at -80°C until use.

Sorption isotherm and state diagram

The lyophilised samples of lactic acid bacteria were reduced in powder in a chamber of very low relative humidity (less than 5%) and then put in the containers used for the measurement of water activity. The containers were placed in hermetic glass box containing P₂O₅ or saturated salt solutions with water activities indicated in Table 1. After one week of equilibration at 25°C, the samples reached a constant weight and the target water activity. Water content was determined by the Karl Fisher titration method using a Metrohm KF 756 apparatus (Herisau, Switzerland), the water activity of the samples was measured at 25°C using an aw-meter labMasteraw (Novasina, Precisa, Poissy, France) and the glass transition temperature was determined by differential scanning calorimetry (DSC) (Perkin Elmer LLC, Norwalk, CT, USA) as previously described [18].

Desorption experiments

Desorption kinetics were followed using the weighing system (microbalance) CWS-40 of Martin-Christ (Osterode an Harz, Germany). The accuracy of the balance was ±0.005g according to manufacturer data. The balance and its operation have been fully described before [37]. An offset alignment was performed before each run throughout the study. The microbalance was placed in the centre of the middle shelf. The weighted vial was protected from radiation from the chamber walls and door by surrounding it with additional vials filled with freeze-dried product. A user-defined weighing interval of 5 min was used throughout this work. The lifting and weighting step took less than 10s, after which the vial was lowered back on the shelf and released from the holding arm. The duration of interruption of heat transfer between the shelf and the vial caused by weighing was therefore less than 4% of the total duration of experiment.

Samples of bacterial suspension freeze-dried in 7 mL glass vials were equilibrated at a relative humidity of 33% at 25°C (using MgCl₂•6H₂O saturated solution). The vial was then introduced in the microbalance device placed on a pre-heated or pre-cooled shelf of the SMH 90 freeze dryer (15°C, 25°C or 35°C). The cold trap of the freeze-dryer was pre-cooled at -65°C. Once the vial was transferred to the microbalance, the chamber pressure was decreased to its minimal value and the data acquisition of the microbalance was started using Christ's software. The experiments were stopped after 10 or 24 hours of desorption at 15, 25 or 35 °C. Temperature was given by the sensor build into the microbalance. It was not possible to place thermocouples inside the product because it was already solid (freeze-dried and equilibrated at 33% relative humidity) at the beginning of desorption experiments and because mechanical forces induced by wires would have disturbed the

weighting process. The water content and the water activity were determined at the initial and final times of the experiments. The experiments were repeated in identical operating conditions but using an empty vial in order to compensate the weight variation measurement with temperature.

Dynamic desorption model

Sorption isotherm

At the end of the primary drying step, ice has been removed by sublimation but the product still contains unfrozen water bound to the solid matrix. Let X be the moisture content of the product in kg water per kg of product (wet basis):

$$\text{Eq. 1} \quad X = \frac{m_w}{m_w + m_s}$$

The equilibrium moisture content at a given water activity (a_w) was expressed by the frequently used Guggenheim-Anderson-Boer (GAB) formula:

$$\text{Eq. 2} \quad X^{equ} = \frac{X_M K C a_w}{(1 - K a_w)(1 + K a_w(C - 1))}$$

In this equation, X_M represents the monolayer moisture content while K and C are dimensionless shape coefficients.

Desorption kinetics

Early studies[19, 20] showed that in biological products water may exist in several physical states such as monolayer, multilayer, cluster of water molecules or liquid. Water in each state is more or less tightly bound to the solid matrix, and it was experimentally shown that moisture fractions in different physical states have different desorption kinetics.[21] For generality, the model is given for any number n of such “compartments”. One, two or three compartments were used when running the model, as further described in the results section. Denote m_{wi} the water mass in compartment i :

$$\text{Eq. 3} \quad \sum_{i=1}^n m_{wi} = m_w$$

Partial moisture contents corresponding to each compartment were defined as:

$$\text{Eq. 4} \quad X_i = \frac{m_{wi}}{m_w + m_s}$$

with

$$\text{Eq. 5} \quad \sum_{i=1}^n X_i = X$$

The desorption rate is usually assumed proportional either to the current moisture content[25, 34, 36, 38, 39] or to the difference between the current and the equilibrium moisture content.[3, 5, 6, 8, 9, 26, 31, 28] In principle, the former should be reserved to non water-binding materials such as mannitol which forms anhydrous crystals upon lyophilisation and whose equilibrium moisture content is essentially zero,[15] while the latter should be used for water-binding materials like most amorphous biological formulations. In practice, however, neglecting the equilibrium moisture content for water-binding materials (e.g. skim milk) can lead to satisfactory model predictions if the equilibrium moisture content is much lower than the lowest one achieved in the considered experiments.[2, 23, 30, 40] In this work, since a water-binding material was used, the expression

including the equilibrium moisture content was considered for generality. For each compartment this gives:

$$\text{Eq. 6} \quad \frac{dX_i}{dt} = \frac{1}{\tau_i} (X_i^{equ} - X_i)$$

with τ_i being the characteristic desorption time for water in physical state i .

In steady state operating conditions, i.e. constant temperature and vapour pressure, the equilibrium moisture content X_i^{equ} and the characteristic desorption times τ_i are constant and the above equation has the solution:

$$\text{Eq. 7} \quad X_i(t) = X_i^{equ} + (X_i^{ini} - X_i^{equ}) e^{-\frac{t}{\tau_i}}$$

In time-varying conditions, X_i^{equ} and τ_i depend on time and the solution is slightly more complex:

$$\text{Eq. 8} \quad X_i(t) = e^{b(t)} X_i^{ini} + \int_0^t \frac{X_i^{equ}(\theta)}{\tau_i(\theta)} e^{b(t)-b(\theta)} d\theta$$

with

$$\text{Eq. 9} \quad b(t) = \int_0^t \frac{-1}{\tau_i(\theta)} d\theta$$

In practice, the initial and the equilibrium moisture contents are determined (measured or calculated using the sorption isotherm) for the product as a whole. To define the distribution of water among the compartments, it was assumed that, at equilibrium, the compartments containing most strongly bound water are filled before compartments corresponding to a less bound water state. Each compartment can contain a certain maximum amount of moisture (X_i^{max}). For example, in the two-compartment model considered below, the available amount of moisture will fill the monolayer (compartment 1) up to the maximum amount $X_1^{max} = X_M$ given by the GAB sorption isotherm (Eq. 2) and the remaining moisture will be in the multilayer (compartment 2).

Mathematically, these considerations were formalized as follows. The compartments were ordered by decreasing degree of water binding, which, in the context of this study, corresponds to decreasing characteristic desorption times:

$$\text{Eq. 10} \quad \tau_1 > \tau_2 > \dots > \tau_n$$

The assumption of successive compartment filling up to a maximum moisture content was expressed by the following equation applied to each compartment i :

$$\text{Eq. 11} \quad X_i^{equ} = \max\{0, \min\{X_i^{max}, X^{equ} - \sum_{k=1}^{i-1} X_k^{max}\}\}$$

Here X^{equ} is the equilibrium moisture content of the whole product as given by the sorption isotherm and the sum represents the total moisture content that can be stored in the ‘previous’ compartments ($k < i$). Formally, this sum is considered zero for the first compartment ($i=1$).

As an example, consider the application of this rule to the two-compartment model ($n=2$, $i=1$ monolayer, $i=2$ multilayer, $X_1^{max} = X_M$):

273 Eq. 12
$$\begin{aligned} & \text{if } X^{equ} < X_M, \text{ then } X_1^{equ} = X^{equ} \text{ and } X_2^{equ} = 0 \\ & \text{if } X^{equ} \geq X_M, \text{ then } X_1^{equ} = X_M \text{ and } X_2^{equ} = X^{equ} - X_M \end{aligned}$$

274 Thus at equilibrium, if the total moisture content of the product is lower than X_M , the whole amount
275 of water will be contained in the monolayer. If it is higher, the monolayer will contain X_M and the
276 remaining amount will be in the multilayer, as physically expected.

277 The application of the considered rule for a model with n compartments introduces $n - 1$ model
278 parameters, namely the maximum moisture contents $X_1^{max} \dots X_{n-1}^{max}$. The maximum moisture content
279 of the 'last' (less bound water) compartment (X_n^{max}) needs not to be specified since this
280 compartment will contain the remaining water not stored in the previous compartments. In the case
281 of the two-compartment model considered below (monolayer and multilayer), there are actually no
282 additional model parameters to be determined since the maximum moisture content of the
283 monolayer ($X_1^{max} = X_M$) is already given by the GAB formula (Eq. 2).

284 The initial moisture content in each compartment (X_i^{ini}) was calculated by Eq. 13 similar to Eq. 11,
285 because, according to the experimental protocol, the product moisture was at equilibrium at the
286 beginning of the experiments:

287 Eq. 13
$$X_i^{ini} = \max\{0, \min\{X_i^{max}, X^{ini} - \sum_{k=1}^{i-1} X_k^{max}\}\}$$

288 Of course, the simplifying modelling assumption leading to Eq. 11 and Eq. 13 is only a schematic
289 view of physical reality. It is expected to be reasonable, however, if the degrees of water binding are
290 significantly different among the compartments, which can be assessed, for example, by large
291 differences in characteristic desorption times (τ_i). These considerations are quantitatively verified in
292 the Results section.

293 Finally, in order to use gravimetric measurements for model fitting, the moisture content was used
294 to express the mass measured by the balance, which includes the mass of solid matrix (m_s), water
295 (m_w) and vial (m_v):

296 Eq. 14
$$m = m_s + m_w + m_v = m_s \frac{1}{1-X} + m_v$$

297

298 Temperature dependence

299 It is common practice in freeze-drying to increase shelf temperature in the secondary drying stage in
300 order to accelerate desorption. In the considered desorption model (Eq. 8), temperature dependent
301 parameters are the equilibrium moisture content (X^{equ}) and the characteristic desorption times (τ_i). In
302 usual freeze-drying conditions the equilibrium moisture content is very close to zero and its
303 variations have only a minor impact on the desorption kinetics; it was thus taken as constant. In this
304 study, temperature dependence was assumed for the characteristic desorption times via an
305 Arrhenius-like relationship [25, 30]:

306 Eq. 15
$$\tau_i = \tau_i^{ref} e^{-\frac{E_{ai}}{R} \left(\frac{1}{T} - \frac{1}{T^{ref}} \right)}$$

307 This form is mathematically equivalent to the classical Arrhenius formula but has the advantage that
308 the pre-exponential factor has a straightforward physical meaning: τ_i^{ref} represents the value of the

characteristic desorption time at the arbitrarily fixed reference temperature T^{ref} . The activation energy (E_{ai}) expresses the temperature sensitivity of the characteristic desorption time.

Model parameter identification

Desorption model parameters were determined in two steps. In the first step, the parameters of the GAB sorption isotherm (X_M , C , K) were determined by fitting Eq. 2 in a least-square sense to experimentally measured data of moisture content (X) for various values of water activity (a_w).

In the second step, desorption kinetic parameters were determined by fitting simultaneously moisture content values given by Eq. 8 and Eq. 5 and total mass values given by Eq. 14 to experimental measurements from 6 experiments performed at 3 different temperatures between 15 and 40°C and different initial moisture contents in the range 0.05 to 0.07 kg/kg. In the fitting process, some of the parameters were considered product-dependent and thus taken as common to all 6 experiments: reference time constants (τ_i^{ref}) and activation energies (E_{ai}). The other parameters had to be taken as specific to each experimental run and thus separate values for each experiment were determined: initial mass of the solid product in a vial (m_s), mass of the vial (m_v) and initial moisture content (X^{ini}). Since all moisture content measurements are affected by statistically equivalent measurement errors, the initial moisture content of an experiment was not forced to the first measured value but considered as an unknown parameter to be determined in the model fitting process.

As measurements of different physical nature (mass and moisture content) were used simultaneously in least-squares fitting, relative weights had to be affected to each type of measurement. Selection of weights accounts for several factors, such as numerical range of each type of measurement, relative accuracy and relative frequency. In the considered case numerical ranges of both variables were comparable (of order of 0.05 g of mass variation and 0.05 kg/kg of moisture content variation) but mass measurements were more frequent and more accurate. After some tests, a twice higher weight for the moisture content was found adequate to balance lower frequency combined with lower accuracy.

Numeric calculations were performed with Matlab™ 8 software (The MathWorks Inc., Natick, MA) equipped with the Statistics Toolbox.

Results and Discussion

Equilibrium moisture content

The GAB sorption isotherm given by Eq. 2 was fitted to 29 experimental measurements of moisture content, in the range of 0.02 to 0.92 water activity. The resulting equilibrium moisture content is given in Figure 1 as a function of the water activity, together with the experimental data used for parameter identification. The GAB model appears to fit experimental data satisfactorily (residual standard deviation less than 0.013 kg/kg), the largest error (0.03 kg/kg) being around $a_w = 0.53$. Determined GAB model parameters and their standard errors are given in Table 2. The monolayer moisture content (X_M) and the parameter K could be determined accurately with the available measurements, with a coefficient of variation less than 10%. A relatively large uncertainty remains about the value of the shape parameter C , as measured by its standard error, because Eq. 2 is less sensitive to the value of this parameter.

Desorption kinetics

Models with $n = 1, 2$ and 3 compartments (physical states of bound water) were tested to represent experimentally measured desorption kinetics. The single compartment model clearly failed to describe the observed sample mass evolution (Figure 2, dotted lines). Predicted mass decrease was too slow at the beginning of the experiments compared to the experimental one, and too fast towards the end. The prediction of the final moisture content was also inadequate in many cases, as in Figure 2B. These observations supported the assumption that in the considered samples, water was present in at least two states with different desorption kinetics.

The two-compartment model was found to represent experimental data adequately. As an example, Figure 2 shows model simulation results together with measured sample mass and moisture content values for two experiments, performed at extreme temperatures in the considered range. Two different drying kinetics, a fast initial one (roughly before 3h) and a much slower subsequent one, are clearly visible from high frequency mass measurements and are correctly reproduced by the considered model. The equilibrium moisture content of the samples, as given by the sorption isotherm, always remains far below the current values (Figure 2, dash-dotted line), explaining why desorption models with zero equilibrium moisture content were successfully used in freeze-drying even for water binding materials.[25, 34, 36, 38, 39] It is also apparent from Figure 2 that higher temperature accelerates desorption, as expected. Sample temperature was not perfectly constant in these experiments, justifying the use of Eq. 8 instead of Eq. 7 for model simulation.

Determined desorption model parameters are reported in Table 3. The reference temperature for calculation of the characteristic desorption times in Eq. 15 was arbitrarily fixed to $T^{ref} = 273.15$ K (0°C). According to Eq. 13, the initial moisture content of the first compartment (slowest desorption) was fixed to the monolayer moisture content determined for the GAB equation ($X_1^{ini} = X_M$, Table 2). The initial moisture content of the second compartment (fast desorption) was calculated as the difference to the total initial moisture content of the product ($X_2^{ini} = X^{ini} - X_1^{ini}$). Note that product samples had slightly different initial moisture contents in each of the 6 desorption experiments, in the range 0.056 to 0.069 kg/kg w.b; accordingly, the considered X_2^{ini} was specific to each experimental run.

It appears from Table 3 that the characteristic desorption times for the two compartments are quite different, by a factor of almost 30 (92.5 and 3.2h respectively at the reference temperature). This suggests that two distinct forms of bound water are involved, with different binding strengths to the solid matrix. In the considered moisture content range, these forms of bound water can be ascribed to the monolayer and multilayer or water molecules clustered around polar groups [19, 20]. Adequate model fit was achieved by fixing the initial moisture content of the slowly desorbing compartment to the value of the monolayer given by the GAB sorption isotherm, comforting the hypothesis that the slowly desorbing compartment corresponds to the monolayer and the quickly desorbing one to the multilayer. In the literature, several studies reported specific water desorption rates for the secondary stage of the freeze-drying process, which represent the inverse of the characteristic desorption times used in Eq. 6: $11 \times 10^{-5} \text{ s}^{-1}$ (i.e. $\tau = 2.52$ h) for skim milk [31], $7.8 \times 10^{-5} \text{ s}^{-1}$ (i.e. $\tau = 3.56$ h) also for skim milk [32, 40, 39], $7.9 \times 10^{-5} \text{ s}^{-1}$ (i.e. $\tau = 3.5$ h) for sucrose and $9.6 \times 10^{-5} \text{ s}^{-1}$ (i.e. $\tau = 2.9$ h) for polyvinylpyrrolidone [5]. All these values are close to the fastest desorption time constant found in this study ($\tau_2^{ref} = 3.2$ h), suggesting that models described in the literature usually refer to the desorption of the water in the multilayer. A model based solely on this fast time constant

might be substantially in error if applied down to moisture contents close to or below the monolayer, which might be the case for the target moisture contents of some freeze-dried products. This can lead to underestimation of the final moisture content of the product and jeopardize its subsequent stability.

It was found that a common value of the activation energy for both compartments (Table 3) adequately described the temperature dependence of both desorption kinetics (Eq. 15). Considering a common activation energy led to a simpler model and smaller uncertainty (standard error) in parameter values. The value of the activation energy for the desorption kinetic determined in our experiments (28.7 kJ/mol, Table 3) is product-dependent and was found somewhat lower than values reported in the literature: 37.7 kJ/mol for sucrose,[30] 79.4 kJ/mol for moxalactam di-sodium [21]. Many previous studies, however, did not take into account the temperature dependence of the desorption kinetic constant and considered a fixed value for this parameter, which is formally equivalent to zero activation energy.[5, 6, 23, 26, 31, 36] Some authors use quite different desorption time constants between primary and secondary drying, that may indirectly account for the temperature effect, since in secondary drying the product temperature is typically 30 to 60°C higher than in the primary drying. For instance, several studies[32, 39, 40] use a desorption kinetic constant of $6.48 \times 10^{-7} \text{ s}^{-1}$ (i.e. $\tau = 428.7 \text{ h}$) for the primary drying and $7.8 \times 10^{-5} \text{ s}^{-1}$ (i.e. $\tau = 3.56 \text{ h}$) for the secondary drying of skim milk. For the present study, temperature dependence of the characteristic desorption times of the two compartments is given in Figure 3. The general shape of the two curves is the same because the same activation energy was considered. It appears from Figure 3 that in the usual temperature range encountered in freeze-drying, desorption is more than 3 times faster at 40 than at 10°C.

A model with three compartments (three distinct physical states of the water) was also tested, but not retained for several reasons. Firstly, the model fit improvement was minor; the residual standard deviation decreased by less than 6% compared to the two compartment model. Secondly, in the considered range of moisture contents (below 0.07 kg/kg) it is unlikely that bound water could be found in another state than monolayer or multilayer, such as condensed in pores or capillaries. Figure 1 suggests that less bound forms of water could exist only above 0.1 or 0.2 kg/kg for this product.[20, 41] Finally, the determined characteristic desorption time constant of the third (fastest desorbing) compartment at the reference temperature (τ_3^{ref}) was slightly above 1h, of the same order as τ_2^{ref} in Table 3. It is thus questionable whether this might indicate a distinct state of water in the solid matrix.

In summary, the two compartment model appeared to present the best compromise between fit to experimental data and physical significance.

Conclusion

A model for the equilibrium moisture content and for the desorption kinetics of freeze-dried lactic acid bacteria preparation was developed. Two distinct desorption kinetics were observed, which could be assimilated to water in monolayer (slow desorption) and multilayer (fast desorption). Temperature effect on the desorption kinetics was included in the model, showing a three-fold decrease of the characteristic desorption time between 10 and 40°C. The developed model is intended to be used in the design and optimisation of freeze-drying protocols, where the desorption time to reach moisture content close to or lower than monolayer can take a significant fraction of the

total freeze-drying time. Accurate prediction of the final moisture content avoids under-drying as well as over-drying, which are both detrimental to product stability.

Acknowledgement

The research leading to these results has received funding from the European Community's Seventh Framework Programme (FP7/2007-2013) under grant agreement CAFE n° KBBE-212754.

References

- 1 Tang, X.; Pikal, M. J. Design of freeze-drying processes for pharmaceuticals: practical advice. *Pharmaceutical Research*, 2004, 21(2),191–200.
- 2 Sadikoglu, H.; Ozdemir, M.; Seker, M. Freeze-drying of pharmaceutical products: Research and development needs. *Drying Technology*, 2006, 24(7),849–861.
- 3 Sadikoglu, H.; Liapis, A. I.; Crosser, O. K. Optimal control of the primary and secondary drying stages of bulk solution freeze drying in trays. *Drying Technology*, 1998, 16(3-5),399–431.
- 4 Boss, E. A.; Filho, R. M.; de Toledo, E. C. V. Freeze drying process: real time model and optimization. *Chemical Engineering and Processing*, 12 2004, 43(12),1475–1485.
- 5 Trelea, I. C.; Passot, S.; Fonseca, F.; Marin, M. An interactive tool for freeze-drying cycle optimisation including quality criteria. *Drying Technology*, 2007, 25,741–751.
- 6 Velardi, S. A.; Barresi, A. A. Development of simplified models for the freeze-drying process and investigation of the optimal operating conditions. *Chemical Engineering Research & Design*, 2008, 86(A1),9–22.
- 7 Pisano, R.; Fissore, D.; Velardi, S. A.; Barresi, A. A. In-line optimization and control of an industrial freeze-drying process for pharmaceuticals. *Journal of Pharmaceutical Sciences*, 2010, 99(11),4691–4709.
- 8 Antelo, L. T.; Passot, S.; Fonseca, F.; Trelea, I. C.; Alonso, A. A. Toward optimal operation conditions of freeze-drying processes via a multilevel approach. *Drying Technology*, 2012, 30(13),1432–1448.
- 9 Sadikoglu, H.; Ozdemir, M.; Seker, M. Optimal control of the primary drying stage of freeze drying of solutions in vials using variational calculus. *Drying Technology*, 2003, 21(7),1307–1331.
- 10 Chouvinc, P.; Vessot, S.; Andrieu, J.; Vacus, P. Optimization of the freeze-drying cycle: a new model for pressure rise analysis. *Drying Technology*, 2004, 22(7),1577–1601.
- 11 Schoug, A.; Olsson, J.; Carlfors, J.; Schnurer, J.; Hakansson, S. Freeze-drying of lactobacillus coryniformis si3—effects of sucrose concentration, cell density, and freezing rate on cell survival and thermophysical properties. *Cryobiology*, 2006, 53(1),119–127.
- 12 Tang, X.; Nail, S. L.; Pikal, M. J. Evaluation of manometric temperature measurement, a process analytical technology tool for freeze-drying: part i, product temperature measurement. *AAPS PharmSciTech*, 2006, 7(1),E14.

- 470 13 Passot, S.; Trelea, I. C.; Marin, M.; Galan, M.; Morris, G.; Fonseca, F. Effect of controlled ice
471 nucleation on primary drying stage and protein recovery in vials cooled in a modified freeze-
472 dryer. *Journal of Biomechanical Engineering - Transactions of the ASME*, 2009, 131,0745111–
473 5.
- 474 14 Shalaev, E. Y.; Zografi, G. How does residual water affect the solid-state degradation of drugs
475 in the amorphous state. *Journal of Pharmaceutical Sciences*, 1996, 85,1137–1141.
- 476 15 Costantino, H. R.; Curley, J. G.; Hsu, C. C. Determining the water sorption monolayer of
477 lyophilized pharmaceutical proteins. *Journal of Pharmaceutical Sciences*, 1997, 86,1390–
478 1393.
- 479 16 Precausta, P.; Genin, N.; Benet, G.; Tourneur, N. Freeze-drying/Lyophilization of
480 pharmaceutical and biological products, volume 96, chapter Industrial freeze-drying of
481 vaccines destined for veterinary purposes : an overview, pages 337–357. Marcel Dekker, New
482 York, 1999.
- 483 17 Zayed, G.; Roos, Y. H. Influence of trehalose and moisture content on survival of *Lactobacillus*
484 *salivarius* subjected to freeze-drying and storage. *Process Biochemistry*, 2004, 39,1081–1086.
- 485 18 Passot, S.; Cenard, S.; Douania, I.; Trelea, I. C.; Fonseca, F. Critical water activity and
486 amorphous state for optimal preservation of lyophilized lactic acid bacteria. *Food Chemistry*,
487 2012, 132,1699–1705.
- 488 19 Karel, M. Water Relations of Foods. *Food Science and Technology* (a series of monographs),
489 chapter Physico-chemical modification of the state of water in foods - A speculative survey,
490 pages 639–657. Academic Press, London, 1975.
- 491 20 Labuza, T. Interpretation of sorption data in relation to the state of constituent water, in
492 *Water Relations of Foods. Food Science and Technology* (a series of monographs), Academic
493 Press, London, 1975; 155–172..
- 494 21 Pikal, M.; Shah, S.; Roy, M.; Putman, R. The secondary drying stage of freeze drying: drying
495 kinetics as a function of temperature and chamber pressure. *International Journal of*
496 *Pharmaceutics*, 1990, 60,203–217.
- 497 22 Liapis, A.; Bruttini, R. A theory for the primary and secondary drying stages of the freeze-
498 drying of pharmaceutical crystalline and amorphous solutes: comparison between
499 experimental data and theory. *Separation Technology*, 1994, 4,144–155.
- 500 23 Sadikoglu, H.; Liapis, A. Mathematical modelling of the primary and secondary drying stages
501 of bulk solution freeze-drying in trays: parameter estimation and model discrimination by
502 comparison of theoretical results with experimental data. *Drying Technology*, 1997,
503 15(3&4),791–810.
- 504 24 Millman, M. J.; Liapis, A. I.; Marchello, J. M. An analysis of the lyophilization process using a
505 sorption-sublimation model and various operational policies. *AIChE Journal*, 1985,
506 31(10),1594–1604.

507 25 Liapis, A. I.; Bruttini, R. Freeze-drying of pharmaceutical crystalline and amorphous solutes in
508 vials - dynamic multidimensional models of the primary and secondary drying stages and
509 qualitative features of the moving interface. *Drying Technology*, 1995, 13(1-2),43–72.

510 26 Sadikoglu, H. Optimal control of the secondary drying stage of freeze drying of solutions in
511 vials using variational calculus. *Drying Technology*, 2005, 23(1-2),33–57.

512 27 Gan, K. H.; Bruttini, R.; Crosser, O. K.; Liapis, A. I. Heating policies during the primary and
513 secondary drying stages of the lyophilization process in vials: effects of the arrangement of
514 vials in clusters of square and hexagonal arrays on trays. *Drying Technology*, 2004,
515 22(7),1539–1575.

516 28 Fissore, D.; Velardi, S. A.; Barresi, A. A. In-line control of a freeze-drying process in vials.
517 *Drying Technology*, 2008, 26(6),685–694.

518 29 Fissore, D.; Pisano, R.; Barresi, A. A. Monitoring of the secondary drying in freeze-drying of
519 pharmaceuticals. *Journal of Pharmaceutical Sciences*, 2011, 100(2),732–742.

520 30 Pisano, R.; Fissore, D.; Barresi, A. A. Quality by design in the secondary drying step of a
521 freeze-drying process. *Drying Technology*, 2012, 30(11-12),1307–1316.

522 31 Mascarenhas, W. J.; Akay, H. U.; Pikal, M. J. A computational model for finite element
523 analysis of the freeze-drying process. *Computer Methods in Applied Mechanics and*
524 *Engineering*, 8/15 1997, 148(1-2),105–124.

525 32 Sheehan, P.; Liapis, A. I. Modeling of the primary and secondary drying stages of the freeze
526 drying of pharmaceutical products in vials: Numerical results obtained from the solution of a
527 dynamic and spatially multi-dimensional lyophilization model for different operational
528 policies. *Biotechnology and Bioengineering*, 1998, 60(6),712–728.

529 33 Nam, J. H.; Song, C. S. Numerical simulation of conjugate heat and mass transfer during
530 multi-dimensional freeze drying of slab-shaped food products. *International Journal of Heat*
531 *and Mass Transfer*, 2007, 50(23-24),4891 – 4900.

532 34 Liapis, A. I.; Bruttini, R. A mathematical model for the spray freeze drying process: The drying
533 of frozen particles in trays and in vials on trays. *International Journal of Heat and Mass*
534 *Transfer*, 2009, 52,100–111.

535 35 Rambhatla, S.; Obert, J.; Luthra, S.; Bhugra, C.; Pikal, M. J. Cake shrinkage during freeze
536 drying: a combined experimental and theoretical study. *Pharmaceutical Development and*
537 *Technology*, 2005, 1,33–40.

538 36 Song, C. S.; Nam, J.; Kim, C.-J.; Ro, S. Temperature distribution in a vial during freeze-drying of
539 skim milk. *Journal of Food Engineering*, 2005, 67(4),467 – 475.

540 37 Roth, C.; Winter, G.; Lee, G. Continuous measurement of drying rate of crystalline and
541 amorphous systems during freeze-drying using an in situ microbalance technique. *Journal of*
542 *Pharmaceutical Sciences*, 2001, 90,1345–1355.

543 38 Cheng, J.; Yang, Z. R.; Chen, H. Q. Analytical solutions for the moving interface problem in
544 freeze-drying with or without back heating. *Drying Technology*, 2002, 20(3),553–567.

545 39 Liapis, A. I.; Bruttini, R. Exergy analysis of freeze drying of pharmaceuticals in vials on trays.
546 *International Journal of Heat and Mass Transfer*, 2008, 51,3854–3868.

547 40 Song, C. S.; Nam, J. H.; Kim, C. J.; Ro, S. T. A finite volume analysis of vacuum freeze drying
548 processes of skim milk solution in trays and vials. *Drying Technology*, 2002, 20(2),283–305.

549 41 Karel, M. Heat and mass transfer in freeze drying, in *Freeze Drying and Advanced Food*
550 *Technology*; Academic Press, New York, 1975; 177 – 202.

551

552 Nomenclature

553

Symbol	Units	Significance
a_w	Pa/Pa	Water activity
C		Shape parameter of the GAB equation
K		Shape parameter of the GAB equation
E_{ai}	kJ/mol	Activation energy for the characteristic desorption time of compartment i
m	kg	Mass recorded by the balance
m_w	kg	Total mass of water in the sample
m_{wi}	kg	Mass of water in state (compartment) i
m_s	kg	Mass of solids in the sample
m_v	kg	Mass of the vial
R	J/(mol K)	Ideal gas constant
t	s	Current time
T	K	Current temperature
T^{ref}	K	Reference temperature
X	kg/kg w.b.	Total moisture content of the sample
X_i	kg/kg w.b.	Moisture content corresponding to state (compartment) i
X^{equ}	kg/kg w.b.	Equilibrium moisture content of the sample
X_i^{equ}	kg/kg w.b.	Equilibrium moisture content for state (compartment) i
X^{ini}	kg/kg w.b.	Initial moisture content of the sample
X_i^{ini}	kg/kg w.b.	Initial moisture content in state (compartment) i
X_M	kg/kg w.b.	Monolayer moisture content
α_i		Fraction of water in state (compartment) i
τ_i	s	Characteristic desorption time of water in state (compartment) i
τ_i^{ref}	s	Characteristic desorption time of water in state (compartment) i at the reference temperature

554

555

556

Tables

Table 1. Water activity of the solutions used for product sample equilibration

Saturated solution	Water activity (Pa/Pa)
P ₂ O ₅	0
LiBr	0.06
ZnBr	0.08
LiCl	0.11
CH ₃ COOK	0.22
MgCl ₂ ·6H ₂ O	0.32
K ₂ CO ₃	0.44
Mg(NO ₃) ₂ ·6H ₂ O	0.53
KI	0.69
NaCl	0.75
KCl	0.84
K ₂ SO ₄	0.97

Table 2. GAB model parameters (value ± standard error) for the equilibrium moisture content

Parameter	Value
X_M (kg/kg w.b.)	0.0433 ± 0.0029
K (–)	0.983 ± 0.007
C (–)	7.78 ± 2.81

Table 3. Dynamic desorption model parameters (value ± standard error)

Parameter	Value
τ_1^{ref} (s)	3.34×10 ⁵ ± 7.61
τ_2^{ref} (s)	1.17×10 ⁴ ± 251
$E_{a1} = E_{a2}$ (kJ/mol)	28.7 ± 0.405

Figures

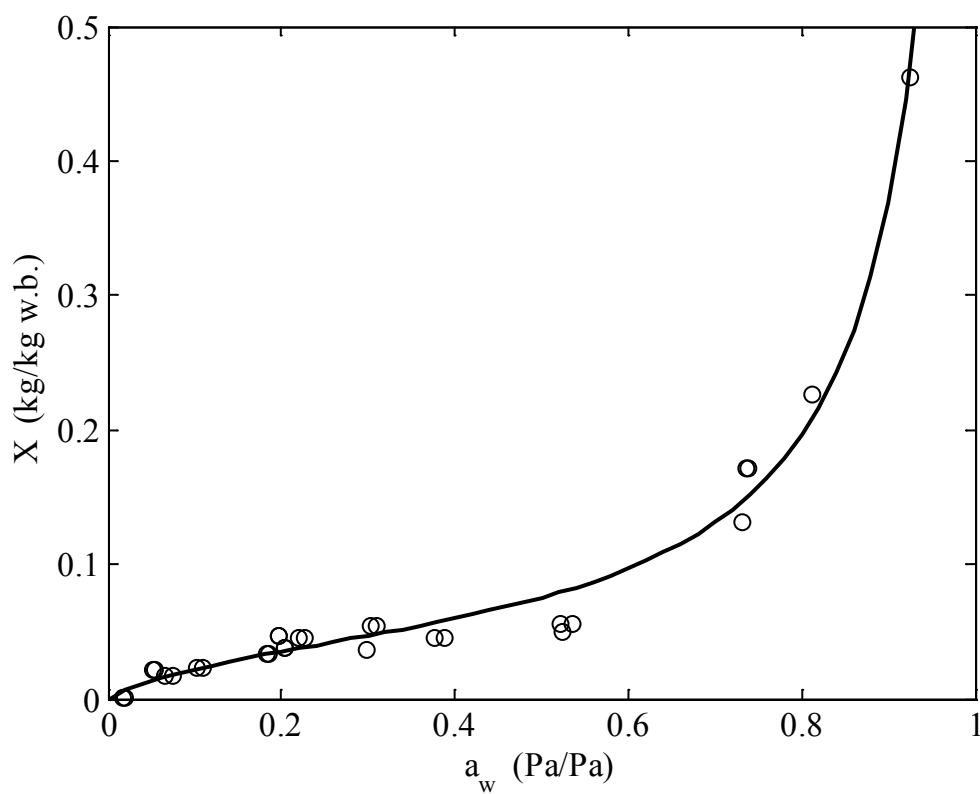


Figure 1. Equilibrium moisture content of the considered product (LAB) as a function of water activity. Symbols: experimental data, solid line: GAB model.

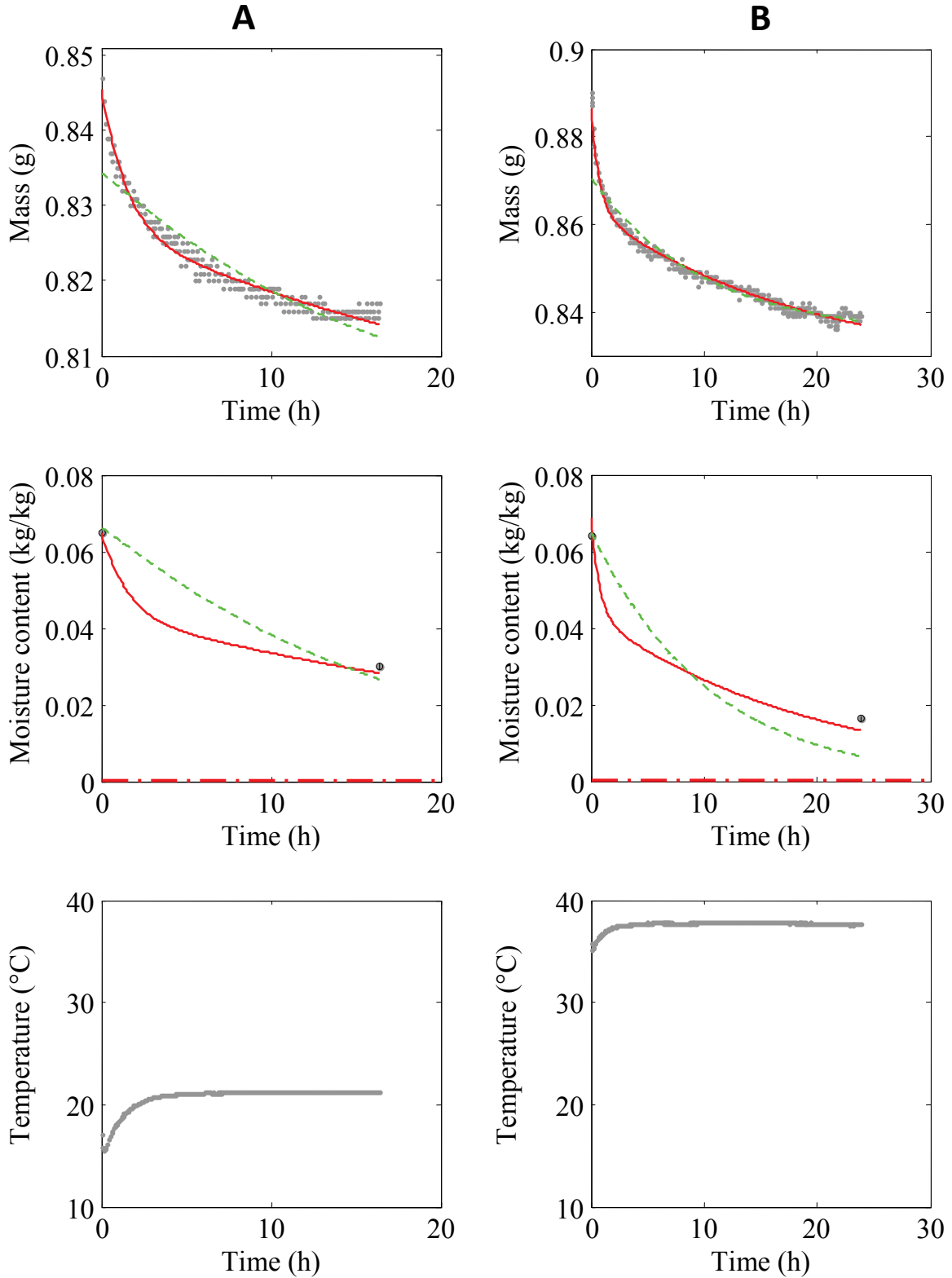
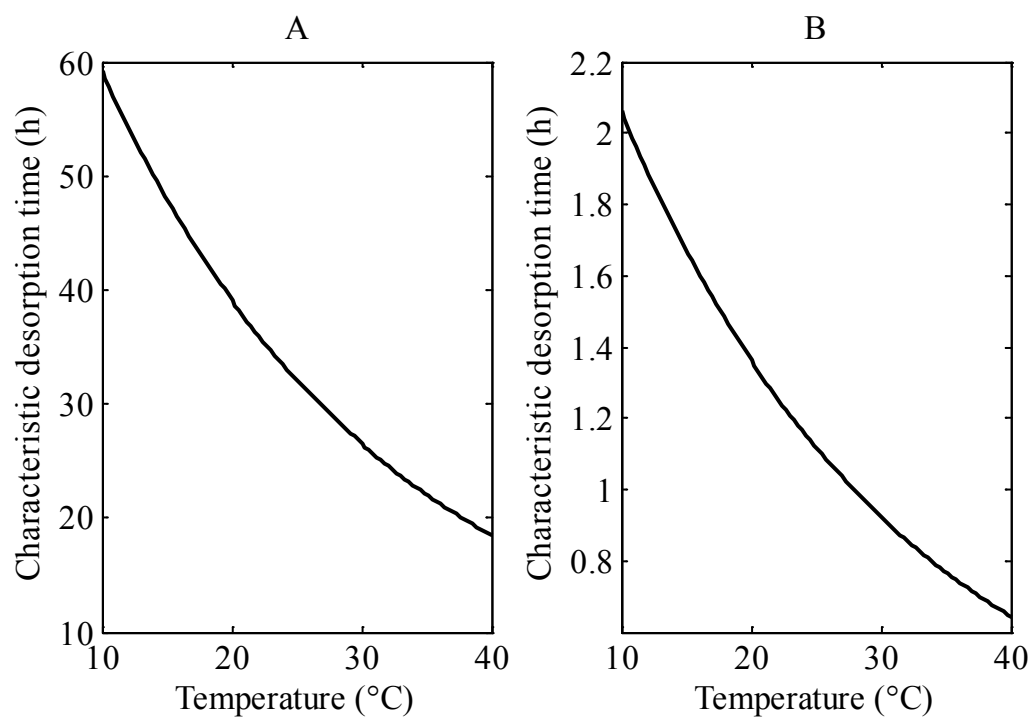


Figure 2. Time evolution of sample mass, moisture content and temperature for two drying experiments. (A) Temperature between 15 and 21°C, (B) between 35 and 38°C. Symbols: experimental data, solid line: 2-compartment model simulations, dotted: 1-compartment model simulations, dash-dotted: equilibrium moisture content (X^{equ}) given by the sorption isotherm.

581



582

583 Figure 3. Characteristic desorption times as function of temperature, in the range of 10 to 40°C.

584 (A) Slowly desorbing water in monolayer. (B) Quickly desorbing water in multilayer.

585

586

587

588